HAL open science

Proteasomal Indoleamine 2,3-Dioxygenase Degradation Reduces the Immunosuppressive Potential of Clinical Grade-Mesenchymal Stromal Cells Undergoing Replicative Senescence

Séverine Loisel, Joelle Dulong, Cédric Menard, Marie-Laure Renoud, Nadine Meziere, Bezier Isabelle, Maelle Latour, Nadège Bescher, Rémy Pedeux, Nicolas Bertheuil, et al.

To cite this version:

Séverine Loisel, Joelle Dulong, Cédric Menard, Marie-Laure Renoud, Nadine Meziere, et al.. Proteasomal Indoleamine 2,3-Dioxygenase Degradation Reduces the Immunosuppressive Potential of Clinical Grade-Mesenchymal Stromal Cells Undergoing Replicative Senescence. Stem Cells / Stem Cells (Miamisburg), 2017, 35 (5), pp.1431-1436. 10.1002/stem.2580 . hal-01516052

HAL Id: hal-01516052

https://univ-rennes.hal.science/hal-01516052

Submitted on 10 Jul 2017

HAL is a multi-disciplinary open access archive for the deposit and dissemination of scientific research documents, whether they are published or not. The documents may come from teaching and research institutions in France or abroad, or from public or private research centers.

L'archive ouverte pluridisciplinaire **HAL**, est destinée au dépôt et à la diffusion de documents scientifiques de niveau recherche, publiés ou non, émanant des établissements d'enseignement et de recherche français ou étrangers, des laboratoires publics ou privés.

Distributed under a Creative Commons Attribution - ShareAlike 4.0 International License

Proteasomal IDO degradation reduces the immunosuppressive potential of clinical grade-mesenchymal stromal cells undergoing replicative senescence

Séverine Loisel[1,2], Joëlle Dulong[1,2], Cédric Ménard[1,2], Marie-Laure Renoud[3], Nadine Meziere[4], Isabelle Bezier[1,2], Maëlle Latour[1,2], Nadège Bescher[1,2], Rémy Pedeux[2], Nicolas Bertheuil[1,2,5], Erwan Flecher[6], Luc Sensebé[3], and Karin Tarte[1,2]

[1] SITI Laboratory, Etablissement Français du Sang Bretagne, CHU Rennes, France

[2] UMR U917, INSERM, Université Rennes 1, Rennes, France

[3] Etablissement Français du Sang Pyrénées Méditerranée, Université Paul Sabatier, UMR5273-INSERM U1031, Toulouse, France

[4] UMR 1348 Pégase INRA, Saint-Gilles, France

[5] Department of Plastic, Reconstructive and Aesthetic Surgery, CHU Rennes, France.

[6] Department of Thoracic and Cardiac Surgery, CHU Rennes, France

RUNNING TITLE: Senescence alters IDO-dependent MSC functions

CORRESPONDENCE:

Karin Tarte, INSERM U917, Faculté de Médecine, 2 Avenue du Pr Léon Bernard, 35043 RENNES, France. e-mail: karin.tarte@univ-rennes1.fr Phone: +33 2 23 23 45 12, fax: +33 2 23 23 49 58

Accepted manuscript

AUTHOR'S CONTRIBUTIONS:

S.L.: collection and assembly of data, data analysis and interpretation, manuscript writing; J.D. and C.M.: collection and assembly of data, manuscript editing; ML.R., N. Ber, and E.F.: collection of human tissues and production of MSCs; N.M.: IDO activity quantification; I.B., M.L., and N.Bes.: collection and assembly of data, final approval of the manuscript; R.P.: final approval of the manuscript; L.S.: financial support, final approval of the manuscript; K.T.: conception and design of the study, financial support, data analysis and interpretation, manuscript writing and final approval.

KEY WORDS: Mesenchymal stem cells. Immunosuppression. Clinical translation. Adipose stem cells. Bone marrow stromal cells. T cells.

Accepted manuscript

ABSTRACT

Owing to their immunosuppressive properties, mesenchymal stromal cells (MSCs) obtained from bone marrow (BM-MSCs) or adipose tissue (ASCs) are considered a promising tool for cell therapy. However, important issues should be considered to ensure the reproducible production of efficient and safe clinical-grade MSCs. In particular, high expansion rate, associated with progressive senescence, was recently proposed as one of the parameters that could alter MSC functionality. In this study, we directly address the consequences of replicative senescence on BM-MSC and ASC immunomodulatory properties. We demonstrate that MSCs produced according to GMP procedures inhibit less efficiently T-cell, but not NK- and B-cell, proliferation after reaching senescence. Senescence-related loss-of-function is associated with a decreased indoleamine-2,3 dioxygenase (IDO) activity in response to inflammatory stimuli. In particular, although STAT-1-dependent IDO expression is transcriptionally induced at a similar level in senescent and non-senescent MSCs, IDO protein is specifically degraded by the proteasome in senescent ASCs and BM-MSCs, a process that could be reversed by the MG132 proteasome inhibitor. These data encourage the use of appropriate quality controls focusing on immunosuppressive mechanisms before translating clinical-grade MSCs in the clinic.

Accepted manuscript

INTRODUCTION

Mesenchymal stromal cells (MSCs) are considered a promising tool for cell-based therapeutic strategies in the context of immune disorders and tissue regeneration [1]. The possibility to expand *ex vivo* high numbers of clinical-grade MSCs from bone marrow (BM-MSCs) or adipose tissue (ASCs) has paved the way for their therapeutic use. In agreement, more than 500 clinical trials evaluating MSC therapy in multiple clinical settings are registered (http://www.clinicaltrials.gov) and encouraging results have been reported in phase I/II trials [1, 2]. Interestingly, the efficacy of transplanted MSCs mainly relies on their paracrine ability to produce trophic factors, reduce inflammation, and dampen innate and adaptive immune response [3, 4]. The increasing use of MSCs and their classification by the Regulatory Authorities as strictly-controlled cell-based medicinal products has led to the development of large-scale standardized production processes [5, 6]. Understanding the main determinants that affect their immunomodulatory activity is crucial for the development of effective MSC strategies. For that purpose, the use of completely defined *in vitro* immunological assays is a pre-requisite to limit uncontrolled technical variability [4, 7, 8].

Besides inter-individual variability, the scale of culture expansion and the related gradual entry into replicative senescence emerge as critical culture-related parameters that could influence clinical-grade MSC safety and clinical efficacy [9, 10]. In particular, late-passage MSCs were shown to be less effective than early-passage MSCs to control acute graft-versus-host disease [11]. More generally, while academic groups essentially use a one-donor to one-recipient strategy with a minimal requirement for *in vitro* amplification, industry-driven trials are based on a one-donor to multiple-recipient strategy and involve MSCs with a high number of cumulative

Accepted manuscript

population doublings (PD) [9]. As senescence is observed in expanding human MSCs [10], it can be hypothesized that long-term culture affects MSC clinical efficacy due to replicative senescence.

Previous analyses of the impact of senescence on MSC immunological properties led to opposite results in relation with the use of unstandardized MSC production processes, senescence induction, and immunological assays [12, 13]. In addition, whereas MSC priming by inflammatory stimuli is a pre-requisite to trigger their suppressive function [14], previous studies regarding MSC senescence only focused on resting MSCs. We investigate here the impact of replicative senescence, induced by long-term culture, on the ability of clinical grade BM-MSCs and ASCs to inhibit immune response. We highlight that senescent MSCs are less efficient than their non-senescent counterpart to inhibit T-cell proliferation and identify the proteasomal degradation of indoleamine 2,3-dioxygenase (IDO) immunosuppressive enzyme as a supportive mechanism.

MATERIALS AND METHODS

Complete Materials and Methods are available in the Supporting Information.

RESULTS AND DISCUSSION

Senescent MSCs display reduced capacity to inhibit T-cell proliferation

To analyze the impact of replicative senescence on immunological properties of MSCs, we maintained clinical-grade MSC batches in culture until senescence and compared paired senescent (SEN+) and non-senescent (SEN-) cells from the same donors.

Accepted manuscript

Reduced cell proliferation occurred after 25-35 cumulative PD for BM-MSCs and 35-45 cumulative PD for ASCs, and was associated with classical senescence features including increased cell size, β-galactosidase (β-gal) staining, and expression of p16INK4 as previously described [10] (Figure S1A-C). To ensure data homogeneity, SEN+ and SEN- MSC batches were defined by a combination of high cumulative PD/β-gal staining >25% *versus* low cumulative PD/β-gal staining <5% (Figure S1D) rather than by the passage number, a highly variable parameter in culture. We then compared the effect of SEN+ and SEN- MSCs on activated purified immune effector cells instead of unfractionated peripheral blood mononuclear cells using robust and validated assays as proposed by the International Society for Cellular Therapy [8, 15]. Interestingly, SEN+ BM-MSCs and ASCs displayed a significantly decreased capacity to inhibit T-cell proliferation compared to their SEN- counterpart regardless of the MSC-to-immune cell ratio although they retained their NK-cell inhibitory function (Figure 1A-B and Figure S2A). SEN- MSCs inhibited T-cell proliferation at a similar level upon transwell coculture (Figure S2B), showing that the mechanism involved was contact-independent. *HGF* and *TGF-β* were significantly upregulated at the mRNA level in ASCs and BM-MSCs during senescence in both resting and inflammatory context, ruling out that the loss of T-cell inhibitory properties of SEN+ MSCs was related to a decreased production of HGF and TGF-β1 soluble immunosuppressive molecules (Figure S2C). The capacity of human MSCs to inhibit T-cell, unlike NK-cell, proliferation *in vitro* was proposed to be dependent on their capacity to express functional IDO [4, 16]. We thus assessed IDO activity of SEN+ versus SEN- MSCs after licensing by weak (20 IU/ml interferon (IFN)-γ; Low IFN) *versus* strong (100 IU/ml IFN-γ +1.5 ng/ml tumor necrosis factor (TNF)-α; Hi IFN +TNF) inflammatory stimuli, as selected by the quantification of IDO mRNA (Figure

Accepted manuscript

1C). Of note, T cells produced similar to higher amounts of IFN-γ and TNF-α when cocultured with SEN+ MSCs compared to SEN- MSCs in agreement with the decreased T-cell suppressive activity of SEN+ MSCs, confirming that the lack of T-cell inhibition by SEN+ MSCs could not be attributed to a weaker inflammatory context (Figure S2D). Interestingly, whereas SEN+ and SEN- MSCs responded to inflammatory cytokines by producing similar amount of IDO mRNA, SEN+ MSCs required a stronger priming than SEN- to trigger a full IDO activity (Figure 1D). In agreement, priming of SEN+ MSCs by a strong inflammatory stimulus restored their capacity to inhibit T-cell proliferation (Figure 1E), even upon cell separation by a transwell (Figure S2B).

Overall these data provide evidences that senescent MSCs are specifically less suppressive towards T-cell immunity than non-senescent MSCs, in association with a reduced IDO activity. Importantly, full senescence was obtained after only 4-9 passages for BM-MSCs *versus* 10-14 passages for ASCs (Figure S1A), indicating that senescence evaluation could be a valuable quality control, in particular for clinical-grade BM-MSCs. In addition, these data strengthen the potential interest of the priming of MSCs with inflammatory stimuli before their clinical use [17].

IDO activity is reduced in senescent MSCs through a proteasome-dependent degradation pathway

Given the discrepancy between IFN-γ-dependent IDO transcription *versus* activity in SEN+ MSCs, we further explored the molecular mechanisms underlying IDO regulation during senescence. We first underlined, through inhibition by validated siRNA (Figure S3) that STAT1 but not STAT3 was required for the induction of IDO transcription by IFN-γ in MSCs (Figure 2A), as described in other cell subsets [18,

Accepted manuscript

19]. STAT1 signaling was retained during MSC senescence (Figure 2B), in agreement with the induction of similar levels of IDO mRNA by IFN-γ in SEN+ *versus* SEN- cells (Figure 1C). We next hypothesized that the decrease of IDO activity during MSC senescence could be due to a decrease of IDO protein stability. In fact, SEN+ MSCs contained less IDO protein than SEN- MSCs after stimulation with weak inflammatory stimuli, a defect corrected by the use of a strong inflammatory priming (Figure 2C). Proteasome has been proposed to regulate IDO protein stability in various cell models [20, 21]. In addition, the proteasome is involved in the regulation of senescence that, in turn, alters the expression of proteasome pathway components [22-24]. We thus tested the MG132 reversible proteasome inhibitor on the inflammation-dependent expression of IDO in MSCs. Interestingly, MG132 specifically increased the amount of IDO protein and activity in SEN+ MSCs (Figure 2D-E), suggesting a crucial role for proteasome degradation pathway in the decrease of IDO activity, and subsequent reduction of immunosuppressive MSC properties during senescence. Identification of IDO-degrading factors and their inducers could provide new quality controls for clinical-grade MSC production as well as new potential targets to maintain IDO-dependent suppressive phenotype.

CONCLUSIONS

Our findings support the emerging idea that senescence modifies MSC immunosuppressive properties. Indeed, our results demonstrate a deleterious effect of senescence on MSC capacity to inhibit T-cell mediated immune response, in link with a proteasome-dependent degradation of IDO. Of note, although resting SEN+ MSCs maintain their ability to sustain B-cell proliferation as previously described for SEN- MSCs [4], priming by weak inflammatory stimuli was sufficient to convert them

Accepted manuscript

into a B-cell suppressive phenotype (Figure S4), suggesting that IDO-independent mechanisms could trigger B-cell inhibition during senescence. These data encourage the definition of accurate qualification controls of MSCs, in particular focusing on immunosuppressive mechanisms, to optimize their use in the clinic.

ACKNOWLEDGMENTS:

This work was supported by grants from the Agence Nationale de la Recherche (ANR-11-RPIB-0012) and the Etablissement Français du Sang (APR 2016), by the Infrastructure program EcellFRANCE (ANR-11-INSB-005), and by the European Center for Transplantation Sciences and Immunotherapy (IHU CESTI, ANR-10-IBHU_0005).

DISCLOSURE OF POTENTIAL CONFLICTS OF INTEREST: The authors indicate no potential conflicts of interest

Accepted manuscript

REFERENCES

1 Uccelli A, Moretta L, Pistoia V. Mesenchymal stem cells in health and disease. Nat Rev Immunol. 2008;8:726-736.

2 Squillaro T, Peluso G, Galderisi U. Clinical Trials With Mesenchymal Stem Cells: An Update. Cell Transplant. 2016;25:829-848.

3 Wang Y, Chen X, Cao W, et al. Plasticity of mesenchymal stem cells in immunomodulation: pathological and therapeutic implications. Nat Immunol. 2014;15:1009-1016.

4 Menard C, Pacelli L, Bassi G, et al. Clinical-grade mesenchymal stromal cells produced under various good manufacturing practice processes differ in their immunomodulatory properties: standardization of immune quality controls. Stem Cells Dev. 2013;22:1789-1801.

5 Sensebe L, Bourin P, Tarte K. Good manufacturing practices production of mesenchymal stem/stromal cells. Hum Gene Ther. 2011;22:19-26.

6 Salmikangas P, Menezes-Ferreira M, Reischl I, et al. Manufacturing, characterization and control of cell-based medicinal products: challenging paradigms toward commercial use. Regen Med. 2015;10:65-78.

7 Menard C, Tarte K. Immunoregulatory properties of clinical grade mesenchymal stromal cells: evidence, uncertainties, and clinical application. Stem Cell Res Ther. 2013;4:64.

8 Krampera M, Galipeau J, Shi Y, et al. Immunological characterization of multipotent mesenchymal stromal cells--The International Society for Cellular Therapy (ISCT) working proposal. Cytotherapy. 2013;15:1054-1061.

9 Galipeau J. The mesenchymal stromal cells dilemma--does a negative phase III trial of random donor mesenchymal stromal cells in steroid-resistant graft-versus-host disease represent a death knell or a bump in the road? Cytotherapy. 2013;15:2-8.

10 Tarte K, Gaillard J, Lataillade JJ, et al. Clinical-grade production of human mesenchymal stromal cells: occurrence of aneuploidy without transformation. Blood. 2010;115:1549-1553.

11 von Bahr L, Sundberg B, Lonnies L, et al. Long-term complications, immunologic effects, and role of passage for outcome in mesenchymal stromal cell therapy. Biol Blood Marrow Transplant. 2012;18:557-564.

Accepted manuscript

12 Sepulveda JC, Tome M, Fernandez ME, et al. Cell senescence abrogates the therapeutic potential of human mesenchymal stem cells in the lethal endotoxemia model. Stem Cells. 2014;32:1865-1877.

13 Zhuang Y, Li D, Fu J, et al. Comparison of biological properties of umbilical cord-derived mesenchymal stem cells from early and late passages: immunomodulatory ability is enhanced in aged cells. Mol Med Rep. 2015;11:166-174.

14 Krampera M. Mesenchymal stromal cell 'licensing': a multistep process. Leukemia. 2011;25:1408-1414.

15 Galipeau J, Krampera M, Barrett J, et al. International Society for Cellular Therapy perspective on immune functional assays for mesenchymal stromal cells as potency release criterion for advanced phase clinical trials. Cytotherapy. 2016;18:151-159.

16 Chinnadurai R, Copland IB, Patel SR, et al. IDO-independent suppression of T cell effector function by IFN-gamma-licensed human mesenchymal stromal cells. J Immunol. 2014;192:1491-1501.

17 Polchert D, Sobinsky J, Douglas G, et al. IFN-gamma activation of mesenchymal stem cells for treatment and prevention of graft versus host disease. Eur J Immunol. 2008;38:1745-1755.

18 Chon SY, Hassanain HH, Gupta SL. Cooperative role of interferon regulatory factor 1 and p91 (STAT1) response elements in interferon-gamma-inducible expression of human indoleamine 2,3-dioxygenase gene. J Biol Chem. 1996;271:17247-17252.

19 Robinson CM, Hale PT, Carlin JM. NF-kappa B activation contributes to indoleamine dioxygenase transcriptional synergy induced by IFN-gamma and tumor necrosis factor-alpha. Cytokine. 2006;35:53-61.

20 Hanafi LA, Gauchat D, Godin-Ethier J, et al. Fludarabine downregulates indoleamine 2,3-dioxygenase in tumors via a proteasome-mediated degradation mechanism. PLoS One. 2014;9:e99211.

21 Orabona C, Pallotta MT, Volpi C, et al. SOCS3 drives proteasomal degradation of indoleamine 2,3-dioxygenase (IDO) and antagonizes IDO-dependent tolerogenesis. Proc Natl Acad Sci U S A. 2008;105:20828-20833.

22 Bertram C, Hass R. Matrix metalloproteinase-7 and the 20S proteasome contribute to cellular senescence. Sci Signal. 2008;1:pt1.

Accepted manuscript

23 Mikawa T, Maruyama T, Okamoto K, et al. Senescence-inducing stress promotes proteolysis of phosphoglycerate mutase via ubiquitin ligase Mdm2. J Cell Biol. 2014;204:729-745.

24 Johmura Y, Sun J, Kitagawa K, et al. SCF(Fbxo22)-KDM4A targets methylated p53 for degradation and regulates senescence. Nat Commun. 2016;7:10574.

Accepted manuscript

FIGURE LEGENDS

Figure 1. Senescent MSCs lose their ability to inhibit T-cell proliferation through IDO activity

(A/B): ASCs (left panels) and BM-MSCs (right panels) were cocultured with either CFSE-labeled purified T-cells stimulated with anti-CD3/anti-CD28 antibodies (MSC to T-cell ratio 1:10) **(A)** or CFSE-labeled purified NK-cells stimulated with IL-2 (MSC to NK-cell ratio 1:1) **(B)**. Inhibition of immune cell proliferation by senescent (SEN+; black symbols) and non-senescent MSCs (SEN-; opened symbols) was assessed by CFSE dilution to determine the proportion of cells that have undergone at least one cell division. Data are expressed as the percentage of proliferating cells after normalization to 100% for the proliferation obtained without MSCs (dotted lines). Six independent ASCs and BM-MSC batches were used. **(C/D):** SEN+ (black symbols) and SEN- (opened symbols) ASCs (circles, n=3) and BM-MSCs (squares, n=4) were stimulated or not with 20 IU/ml IFN-γ (Low IFN) or with 100 IU/ml IFN-γ and 1.5 ng/mL TNF-α (Hi IFN + TNF). Expression of *INDO* (encoding for IDO protein) was measured by RQ-PCR after 24 hours of culture, normalized to 3 housekeeping genes, and represented in arbitrary units obtained by assigning the value of 1 to a pool of PBMC. *IDO* is not detectable in unstimulated MSCs **(C)**; Culture supernatants were collected after 40 hours of culture for IDO activity evaluation through quantification of kynurenine level **(D). (E):** T-cell proliferation inhibition assay was performed using primed MSCs (pMSCs), previously stimulated for 48 hours with Hi IFN + TNF (strong inflammatory priming). Results are represented as in **(A)**. *$p<0.05$; ns: not significant.

Accepted manuscript

Figure 2. IDO protein is degraded by the proteasome in senescent MSCs

(A): SEN- MSCs were transfected with control (siCTL), STAT3 (siSTAT3), or STAT1 (siSTAT1) siRNAs before stimulation by IFN-γ (20 IU/ml). *INDO* expression was measured by RQ-PCR after 24 hours of culture, normalized to 3 housekeeping genes, and represented in arbitrary units obtained by assigning the value of 100 to the siCTL condition. Bars: mean +/- SD from 6 independent experiments (3 with BM-MSCs and 3 with ASCs). *: $p<0.05$; ns: not significant. **(B):** SEN+ and SEN- MSCs were stimulated or not with 20 IU/ml IFN-γ for 45 min. Phospho-STAT1 (pSTAT1) expression was then determined by Western blot and normalized to STAT1. MW: molecular weight. Bars: mean +/- SD from 6 independent experiments (3 with BM-MSCs and 3 with ASCs). ns: not significant. **(C):** SEN+ and SEN- MSCs were stimulated or not for 2 days with 20 IU/ml IFN-γ (Low IFN) or with 100 IU/ml IFN-γ and 1.5 ng/ml TNF-α (Hi IFN + TNF). IDO expression was determined by Western blot and normalized to β-actin. Bars: mean +/- SD from 6 independent experiments (3 BM-MSCs and 3 ASCs). *: $p<0.05$; ns: not significant. **(D)**: SEN+ and SEN- MSCs were stimulated by IFN-γ (20 IU/ml) and exposed to MG-132 or its vehicle, DMSO, for the last 6 hours. IDO expression was determined by Western blot and normalized to β-actin. Bars: mean +/- SD from 6 independent experiments (3 BM-MSCs and 3 ASCs). *: $p<0.05$; ns: not significant. **(E)**: SEN+ and SEN- MSCs were stimulated by IFN-γ (20 IU/ml) in the presence of MG-132 or DMSO, for 2 days. Culture supernatants were collected for IDO activity evaluation through kynurenin quantification. Bars: mean +/- SD from 5 independent experiments (3 BM-MSCs and 2 ASCs). *: $p<0.05$; ns: not significant

Accepted manuscript

Figure S1. MSC characterization

(A): The growth kinetic of BM-MSCs and ASCs was assessed by evaluation of the cumulative population doublings (PD). Shown are the curves obtained for 3 representative BM-MSC and ASC batches. **(B):** Representative β -Galactosidase staining of senescent (SEN+) and non-senescent (SEN-) MSCs. Original magnification x400. **(C)**: *P16* expression was quantified by RQ-PCR in senescent (SEN+) and non-senescent (SEN-) MSCs. P16 transcription level is represented in arbitrary units normalized by assigning the value of 1 to a pool of PBMC for 6 MSCs (3 BM-MSCs and 3 ASCs). **(D):** Criteria used to validate senescent versus non-senescent MSC batches.

Figure S2. Factors involved in the decreased capacity of senescent MSCs to inhibit T-cell proliferation

(**A/B**): SEN+ (black bars) and SEN- (opened bars) MSCs were cocultured either with CFSE-labeled purified T-cells stimulated with anti-CD3/anti-CD28 antibodies or with CFSE-labeled purified NK-cells stimulated with IL-2. Different MSC to immune cell ratios were compared including 1 to 10 and 1 to 25 for T cells (left panel), and 1 to 1 and 1 to 2.5 for NK cells (right panel) (**A**). Inhibition of CFSE-labelled T-cell proliferation by non-stimulated MSCs (left panel) or Hi IFN + TNF-primed MSCs (pMSC, right panel) was also tested at a 1:10 MSC:T-cell ratio in the absence or presence of a transwell (**B**). Inhibition of immune cell proliferation by MSCs was assessed by CFSE dilution to determine the proportion of cells that have undergone at least one cell division. Data are expressed as the percentage of proliferating cells after normalization to 100% for the proliferation obtained without MSCs (dotted lines).

Accepted manuscript

Bars: mean +/- SD from 3 independent experiments (1 BM-MSC and 2 ASCs). (**C**) SEN+ (black symbols) and SEN- (opened symbols) ASCs (circles, n=3) and BM-MSCs (squares, n=3) were stimulated or by IFN-γ (20 IU/ml, Low IFN). *HGF* and *TGFB1* expression was measured by RQ-PCR, normalized to 3 housekeeping genes, and represented in arbitrary units obtained by assigning the value of 1 to SEN- MSCs. *: $p<0.05$ (**D**) Supernatants were collected at the end of activated T-cell culture with and without MSCs and were analyzed by ELISA for IFN-γ (left panel) and TNF-α (right panel) concentrations. Data obtained from 6 independent experiments are shown (3 ASCs and 3 BM-MSCs). ns: not significant, *: $p<0.05$.

Figure S3. Validation of STAT1 and STAT3 siRNA

SEN- MSCs were transfected with control (siCTL), STAT1 (siSTAT1) or STAT3 (siSTAT3) specific siRNAs before stimulation by IFN-γ (20 IU/ml). *STAT1 and STAT3* expression was measured by RQ-PCR 24 hours later, normalized to 3 housekeeping genes, and compared to that obtained with siCTL, arbitrary assigned at 100. Bars: mean +/- SD from 3 independent experiments.

Figure S4. Senescent MSCs efficiently inhibit B-cell proliferation

SEN+ and SEN- MSCs were stimulated or not with 20 IU/ml IFN-γ (Low IFN) or with 100 IU/ml IFN-γ and 1.5 ng/mL TNF-α (Hi IFN + TNF) and were cocultured with CFSE-labeled purified B-cells (MSC to B-cell ratio 1:1) stimulated with CD40L, IL-2, CpG B, and anti-Ig antibodies. Inhibition of B-cell proliferation by SEN+ (black bar) and SEN- (white bar) MSCs was assessed by the CFSE dilution method to determine proportion of cells that have undergone at least one cell division. Data are expressed as the percentage of proliferating cells after normalization to 100% for the

Accepted manuscript

proliferation obtained without MSCs (dotted lines). Bars: mean +/- SD from 3 independent experiments (1 BM-MSCs and 2 ASCs).

Graphical abstract

Clinical-grade mesenchymal stromal cells produced from bone-marrow (BM-MSC) and adipose tissue (ADSC) inhibit T-cell proliferation through their capacity to express functional indoleamine 2,3-dioxygenase (IDO) in response to inflammatory stimuli, in particular IFN-γ and TNF-α, produced by activated T cells (**A**). When they enter replicative senescence (SEN+), a process associated with the production of high number of cells to treat multiple recipients from one donor, both BM-MSC and ADSC lose their T-cell suppressive potential, in association with a proteasome-dependent degradation of IDO (**B**).

Accepted manuscript

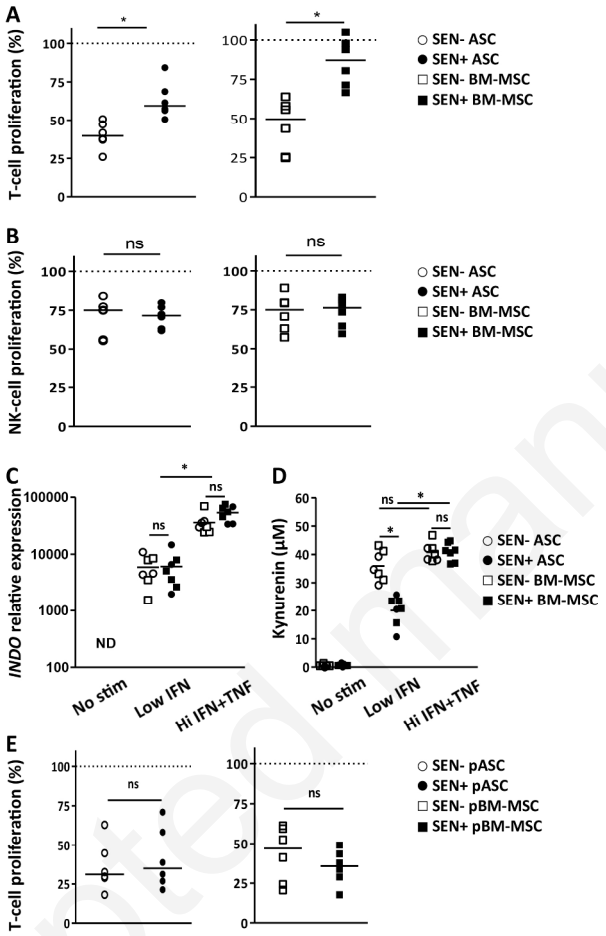

Figure 1. Senescent MSCs lose their ability to inhibit T-cell proliferation through IDO activity
Figure 1.
190x275mm (300 x 300 DPI)

Accepted manuscript

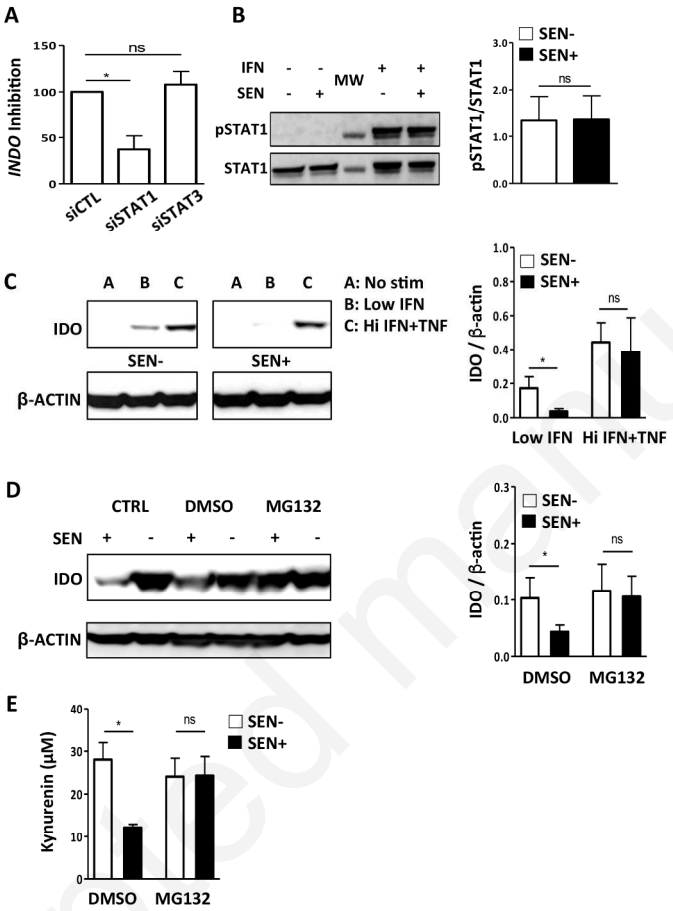

Figure 2. IDO protein is degraded by the proteasome in senescent MSCs
Figure 2.
190x275mm (300 x 300 DPI)

Accepted manuscript

SUPPLEMENTAL METHODS

GMP-grade mesenchymal stromal cells production

Healthy donor recruitment followed institutional review board approval and written informed content process according to the Declaration of Helsinki. Mesenchymal stromal cells (MSCs) were cultured according to GMP principles and following the same process as in our GMP-licensed facility. Briefly, adipose-derived stromal cells (ASCs) were obtained from lipoaspirates after digestion with 0.4 U/mL NB6 collagenase (Roche Diagnostics) for 45 min at 37°C, filtration, and centrifugation to obtain the stromal vascular fraction (SVF) [1]. Cells from the SVF were seeded at 1,000 cells/cm^2 in αMEM supplemented with human platelet lysate (2%), heparin (1 U/ml), penicillin (100 U/ml) and streptomycin (100 µg/ml; Life Technologies). The entire medium was renewed every 3 days until the cells reached near confluence (the end of P0). Cells were then further expanded in the same culture medium at 2,000 cells/cm^2 until senescence. Bone marrow-derived MSCs (BM-MSCs) were obtained as previously reported [2] from unprocessed BM seeded at 5 x 10^4 cells/cm^2 onto CellSTACK in αMEM supplemented with 10% screened FCS (Hyclone), 1 ng/mL FGF-2 (R&D Systems), and 10 µg/mL ciprofloxacin. The entire medium was renewed every 3 days until the cells reached near confluence (the end of P0). Cells were then further expanded in the same culture medium at 1,000 cells/cm^2 until senescence. Phenotypic criteria for MSC definition were validated according to ISCT standards [3] including the expression of CD73, CD105, and CD90 (>90%) and the lack of CD45 (<1%).

When indicated, MSCs were primed (pMSCs) with either 20 IU/ml INF-γ (Low IFN) or with 100 IU/ml IFN-γ and 1.5 ng/ml TNF-α (Hi IFN + TNF; R&D Systems).

Accepted manuscript

Growth kinetic

The growth kinetic was assessed by the number of population doublings (PD). At the end of each passage, PD was calculated as follow: PD = log (number of cells at the end of passage / number of seeded cells) / log2. Since during P_0 MSCs derived from colony-forming unit-fibroblasts (CFU-F), the number of seeded cells corresponded to the number of CFU-F, determined at day 10 of culture as the number of colonies with more than 50 cells. The cumulative PD corresponded to the sum of PD for all passages.

Senescence quantification by detection of β-Galactosidase activity

Senescence of cultivated MSCs was studied by β-Gal staining using the Senescence Detection Kit (BioVision) according to manufacturer's instruction. Total and β-Gal positive cells were enumerated under the microscope.

Real time quantitative PCR (RQ-PCR) analysis

RNA was extracted from MSCs using the RNeasy Micro kit (Qiagen) and cDNA was generated using Superscript II reverse-transcriptase (Invitrogen). For quantitative PCR, assay-on-demand primers and probes, Taqman Universal MasterMix, and ABI Prism 7000 apparatus were used (Applied Biosystems). Gene expression of *IDO, STAT1, STAT3*, *P16, HGF, and TGFB1* was quantified based on the $\Delta\Delta C_T$ calculation method. As previously described, we used *PUM1, CDKN1B* and *EIF2B1* as appropriate housekeeping genes [4]. PCR data were normalized to the geometric mean of these three housekeeping genes. Results were then standardized by comparison to gene expression in a pool of 5 peripheral blood mononuclear cells.

Accepted manuscript

Evaluation of immunosuppressive properties of mesenchymal stromal cells

T-, NK, and B-cells were purified by negative selection from peripheral blood using appropriate Pan T cell (# 130-096-535), NK cell (# 130-092-657), and B cell isolation kits (# 130-091-151; Miltenyi Biotec); respectively. Cell purity was at least 95% as evaluated by flow cytometry. Each immune cell batch was initially validated for its capacity to strongly proliferate without cell death induction in response to their specific stimuli: for T cells, proliferation > 70% and $DAPI^{neg}$ > 60%; for NK cells, proliferation > 70% and $DAPI^{neg}$ > 50%, and for B cells, proliferation > 50% and $DAPI^{neg}$ > 80%. The same controls were repeated in all individual experiments [4]. Each experiment was performed with senescent (SEN+) and non-senescent (SEN-) MSCs from the same donors.

MSCs were seeded at 6 x 10^5 cells/cm^2 corresponding to a confluent monolayer before adding T (ratio of 10T / 1MSC or 25T / 1 MSC), NK (ratio of 1NK / 1MSC or 2.5 NK / 1 MSC), or B cells (ratio of 1B / 1MSC) previously stained with 0.2 µM carboxyfluorescein succinimidyl ester (CFSE) to determine the proportion of $CFSE^{lo}$ dividing cells. T cells were activated for 5 days with 0.5 µg/ml crosslinking anti-CD3 and anti-CD28 antibodies (Sanquin) in RPMI supplemented with 10% screened human AB serum (Eurobio). NK cells were activated for 6 days by 100 IU/ml rhIL-2 (Proleukin, Novartis) in IMDM-10% human AB serum. B cells were activated for 4 days by 50 ng/ml polyhistidine-tagged CD40 ligand and 5 µg/mL anti-polyhistidine antibody (R&D Systems), 1 µg/mL CpG B (ODN 2006, Invivogen), with 5 µg/mL F(ab')2 anti-human IgM/IgA/IgG (Jackson Immunoresearch) in RPMI supplemented with 10% FCS. Alternatively, when indicated, MSCs were seeded on 0.4 µm Transwell insert placed into a microplate well containing activated T cells.

Accepted manuscript

At the end of the coculture, cells were detached by trypsin, stained with PC7-conjugated anti-CD45 antibody (Beckman-Coulter) and DAPI (Sigma-Aldrich) and the proliferation was assessed on viable $DAPI^{neg}CD45^{pos}$ cells using ModFit LT 3.0 software (Verity Software) as the percentage of cells having undergone more than one cell division. The percentage of inhibition of proliferation was defined as follows: (percentage of $CD45^{pos}$ cell proliferation without MSCs - percentage of $CD45^{pos}$ cell proliferation with MSCs) / (percentage of $CD45^{pos}$ cell proliferation without MSCs)*100.

Indoleamine 2,3-Dioxygenase activity

Kynurenine was measured in MSC supernatants by high-performance liquid chromatography (HPLC) using added 3-nitro-L-tyrosine as an internal standard, as previously described [5].

RNA interference experiments

Cells were seeded the day before transfection with control or *STAT1* or *STAT3* specific siRNAs (Life Technologies) using hiPerfect (QIAGEN) following manufacturer's instruction. Culture medium was changed 5 hours later and IFN-γ (20 IU/ml) was added or not to stimulate MSCs.

Western blot

Senescent (SEN+) and non-senescent (SEN-) MSCs were stimulated or not with 20 IU/ml IFN-γ and cell lysates were analyzed by Western blot. Briefly, proteins separated by SDS-PAGE and transferred onto nitrocellulose membranes that were probed with specific antibodies against IDO (Abcam), STAT1, phosphoSTAT1, and β-

Accepted manuscript

actin (Cell Signaling). Proteins of interest were detected and quantified on a G:BOX device (Syngene) with appropriate HRP-conjugated secondary antibodies (Cell Signaling) and visualized with the Pierce ECL Western blotting substrate (Thermo Scientific). In some experiments, 10μM MG132 (Sigma) were added to inhibit proteasome activity 6 hours before performing cell extracts for Western blotting.

Enzyme-linked immunosorbent assay

The production of tumor necrosis factor (TNF)-α and interferon (IFN)-γ in coculture supernatants was measured with enzyme-linked immunosorbent assay (ELISA) kits (R&D, Minneapolis, MN, USA), according to the manufacturer's instructions.

Statistical analysis

Statistical analyses were performed with GraphPad Prism 6.0 software. Comparisons were performed using Wilcoxon test for matched-pairs.

Supplementary Method References

1 Bigot N, Mouche A, Preti M, et al. Hypoxia Differentially Modulates the Genomic Stability of Clinical-Grade ADSCs and BM-MSCs in Long-Term Culture. Stem Cells. 2015;33:3608-3620.

2 Tarte K, Gaillard J, Lataillade JJ, et al. Clinical-grade production of human mesenchymal stromal cells: occurrence of aneuploidy without transformation. Blood. 2010;115:1549-1553.

3 Dominici M, Le Blanc K, Mueller I, et al. Minimal criteria for defining multipotent mesenchymal stromal cells. The International Society for Cellular Therapy position statement. Cytotherapy. 2006;8:315-317.

4 Menard C, Pacelli L, Bassi G, et al. Clinical-grade mesenchymal stromal cells produced under various good manufacturing practice processes differ in their immunomodulatory properties: standardization of immune quality controls. Stem Cells Dev. 2013;22:1789-1801.

5 Tattevin P, Monnier D, Tribut O, et al. Enhanced indoleamine 2,3-dioxygenase activity in patients with severe sepsis and septic shock. J Infect Dis. 2010;201:956-966.

Accepted manuscript

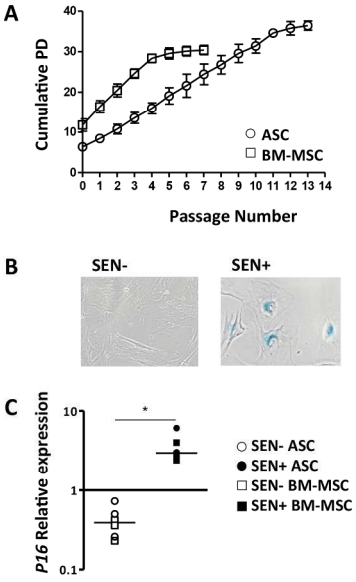

D

	SEN-	SEN+
Cumulative PD	< 20	> 25 for BM-MSC > 35 for ASC
Posβ-Gal (%)	< 5	> 25

190x275mm (300 x 300 DPI)

Accepted manuscript

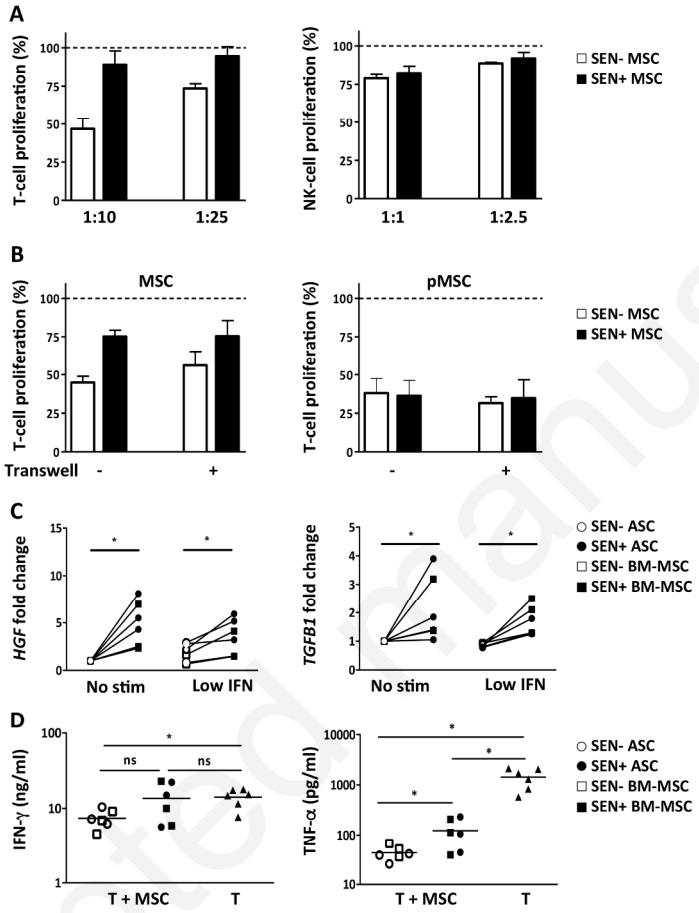

190x275mm (300 x 300 DPI)

Accepted manuscript

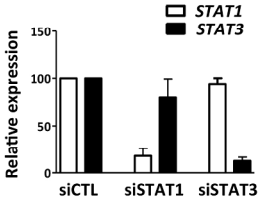

190x275mm (300 x 300 DPI)

Accepted manuscript

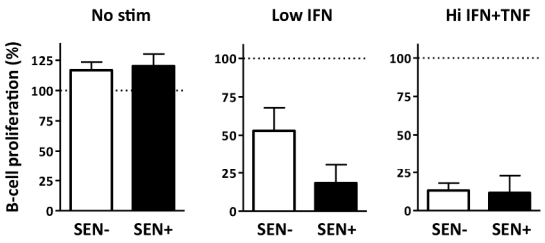

190x275mm (300 x 300 DPI)

Accepted manuscript

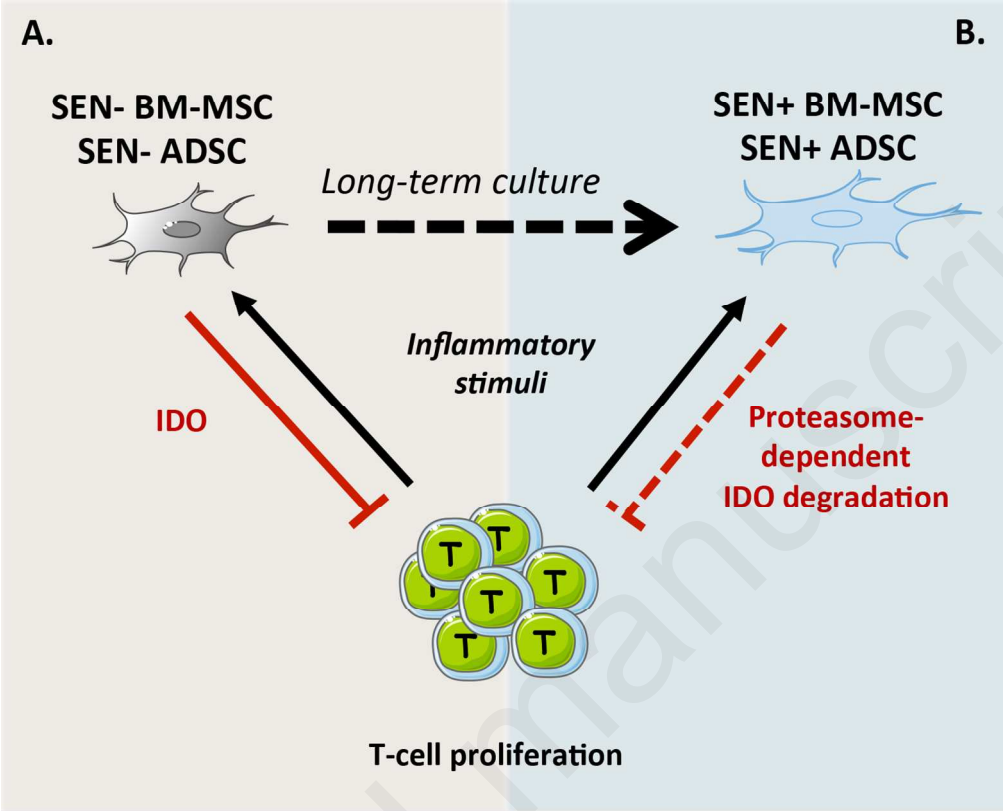

128x103mm (300 x 300 DPI)

Accepted manuscript